



1 *Conference Proceedings Paper*

2 **Spatial variability of daily evapotranspiration in a**
3 **mountainous watershed by coupling surface energy**
4 **balance and solar radiation model with gridded**
5 **weather dataset**

6 **Ricardo Neves de Souza Lima**^{1,*}, **Celso Bandeira de Melo Ribeiro**²

7 ¹ Brazilian Institute of Geography and Statistics, Rio de Janeiro, Brazil; ricardo.s.lima@ibge.gov.br

8 ² Environmental and Sanitary Engineering Department, Federal University of Juiz de Fora, Minas Gerais,
9 Brazil ; celso.bandeira@ufjf.edu.br

10 * Correspondence: ricardo.s.lima@ibge.gov.br; Tel.: +55-21-2142-3649

11 Published: date

12 **Abstract:** The ET determination using ground-based meteorological data does not adequately
13 capture the spatial patterns of mass and energy fluxes in mountainous areas. In this work we
14 evaluate the daily spatial distribution of ET over mountainous watershed in southeastern Brazil, by
15 coupling Surface Energy Balance Algorithms for Land (SEBAL), global solar radiation (GSR) model
16 and a gridded weather dataset (GWD). To estimate daily tilted GSR, we use the relation between
17 terrain and sun angles over 24h integration time. Tests were performed in summer/wet (01/12/2015)
18 and winter/dry (09/25/2015) periods to evaluate the seasonal differences in ET over tilted surfaces.
19 The results indicated different spatial patterns of daily ET on the watershed in each period. In
20 summer, ET was 9.8% higher on slopes facing the South, while in winter ET was 10.6% higher on
21 slopes facing North and East. High variability in daily ET was found on steeper slopes (above 45°),
22 in both periods. The notable ET spatial heterogeneity indicates the complex partitioning of mass and
23 energy fluxes from different terrain angles, which may influence hydro-ecological processes at
24 local scale. The presented approach allowed a more detailed capture of the spatial variability of ET
25 in a mountainous watershed with scarcity ground-based data.

26 **Keywords:** SEBAL; mountainous areas; evapotranspiration.
27

28 **1. Introduction**

29 On mountainous and heterogeneous landscapes the evapotranspiration (ET) estimation using
30 remote sensing becomes more complex due, mainly, to the difficulties to estimate net radiation in
31 different slopes and terrain azimuths, and the uncertainties regarding energy and mass transfer
32 processes, such as advection and local wind flow.

33 Some authors have developed techniques to evaluate the influence of topography on actual ET
34 estimate by remote sensing [1], as well as on reference ET [2] and on surface energy fluxes [3]. In
35 these applications the corrected net radiation for tilted surfaces was obtained from parametrizations
36 using global solar radiation (GSR) modelling, considering different slopes and azimuths of terrain.

37 At watershed scale the ET estimate using ground meteorological stations does not adequately
38 capture the spatial patterns of mass and energy fluxes. The required ground-based meteorological
39 data of the most used remote sensing models for ET retrieval may affect the spatial accuracy,
40 especially in areas with high weather/environmental variability. This issue was addressed by [4]
41 in an approach using raster meteorological data as input to SEBAL model.

42 With the availability of gridded weather datasets (GWD) based on atmospheric reanalysis and
43 numerical weather forecast it became feasible to incorporate the spatialized meteorological
44 information into evapotranspiration models in areas with scarcity ground data. The Global Land
45 Data Assimilation System (GLDAS) represents the state of the art of GWD built using advanced land
46 surface modeling and data assimilation techniques that support several water resources applications
47 [5].

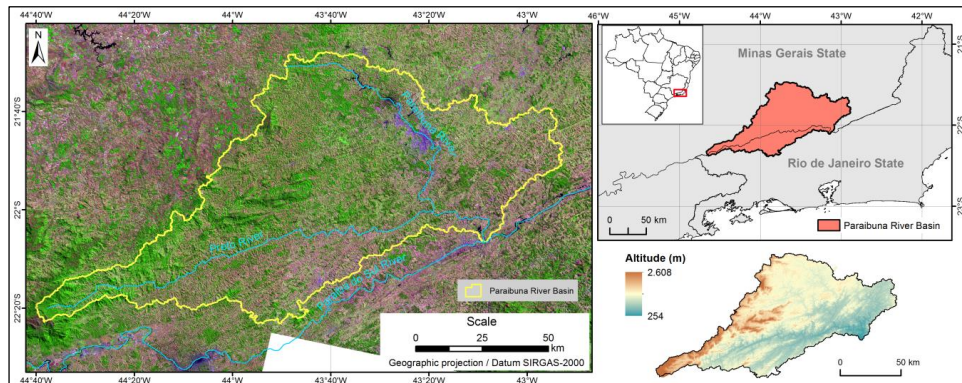
48 In this work we evaluate the daily spatial distribution of ET over a mountainous watershed in
49 southeastern Brazil in summer/wet and winter/dry periods, by coupling Surface Energy Balance
50 Algorithms for Land (SEBAL) and global solar radiation (GSR) model, adapted for tilted surfaces,
51 using the gridded dataset from GLDAS as meteorological input.

52 2. Experiments

53 2.1. Study area

54
55
56

This study area was the Paraibuna watershed, in southeastern region of Brazil (Figure 1).



57
58

Figure 1. Location of the Paraibuna watershed.

59 This watershed is a tributary of the Paraíba do Sul river and covers an area of approximately
60 8,500 km², of which 64% are covered by pasture and croplands, 34% by forests and only 1.2% by urban
61 areas [6]. The regional climate is mild-mesothermic with an annual average temperature of 21°
62 Celsius and total annual rainfall ranging from 1,000 mm to 2,000 mm. Rugged terrain (slope > 25°)
63 occurs in 14% of basin, and altimetric amplitude is about 2,300 meters, with minimum and
64 maximum altitudes of 254 m and 2,608 m, respectively.

65
66

66 2.2. Materials and Methods

67
68
69

68 2.2.1. Datasets

70 Due the studied watershed covers two Landsat-8 scenes, the images were selected from 4 dates,
71 on 12/01/2015 (summer) and 25/09/2015 (close to winter) of path/row 217/75 and 19/01/2015
72 (summer) and 31/08/2015 (winter) of path/row 218/75. Surface reflectance and thermal data was
73 obtained from Landsat Collection Level-1 and Level-2 products, respectively, through EarthExplorer
74 website (<https://earthexplorer.usgs.gov/>). These scenes were selected because of low cloud cover,
75 less than 5%.

76 The input data set used in this study is summarized in Table 1.

77
78

Table 1. General characteristics of input datasets used in the study.

Variable	Unit	Source	Spatial res.	Temporal res.	Provider
Surface reflectance	-	OLI/Landsat-8	30m	16 days	USGS
Thermal radiance	*	TIRS/Landsat-8	30m	16 days	USGS
Altitude	meters	SRTMGL1	30m	-	USGS
Temperature	Kelvin	GLDAS-2.1	~25km	3h	NASA
Specific humidity	Kg/Kg	GLDAS-2.1	~25km	3h	NASA
Wind speed	m/s	GLDAS-2.1	~25km	3h	NASA
Pressure	Pa	GLDAS-2.1	~25km	3h	NASA
Land Cover	class	MAPBIOMAS	30m	Yearly	MAPBIOMAS

* Units in: Watts/(m².srad.μm)

2.2.2. GLDAS data preparation

The 3-hourly GLDAS data were downloaded from GES DISC website (<https://disc.sci.gsfc.nasa.gov/>), covering the same dates of Landsat-8 images. The GLDAS data preparation strategy was composed of three main tasks: 1) Temporal fit to Landsat overpass; 2) Daily aggregation and 3) Spatial resample to 30m resolution.

The temporal fit to Landsat overpass time (aprox. 13 UTC) was performed through a linear interpolation of the GLDAS data at 12h and 15h UTC.

Daily aggregation was performed by simple averaging the 3-hourly GLDAS files per day (8 files) for each variable. The method used for spatial resampling to 30m resolution was the bilinear interpolation. For simplification purposes, spatial downscaling methods were not used.

2.2.3. Solar Radiation Model

To estimate daily tilted GSR (GSR_T), the HDKR (Hay, Davies, Klucher and Reindl) solar radiation model was applied for instantaneous calculations, assuming clear sky conditions, according to [7] and [8]. To estimated the 24-hour average of GSR_T , the instantaneous values computed from 9h to 21h UTC were numerically integrated.

2.2.4. SEBAL model adaptations for tilted surfaces

The implementation of SEBAL, adapted for tilted surfaces, was performed basically by modifications in the Surface albedo (α), Incoming shortwave radiation (R_{S_i}) and surface temperature (T_s), as described next. These parameters are critical inputs in energy balance formulations. Details about theoretical and operational steps to compute each component of energy balance equation in SEBAL can be found in [9].

The surface albedo (α) was computed through the integration of OLI/Landsat-8 surface reflectance bands using the approach described in [10]. This approach was applied over the terrain corrected OLI bands by the SCS+C algorithm [11] to derive the topographically corrected surface albedo (α_T).

The incoming shortwave radiation (R_{S_i}) used in SEBAL was the instantaneous tilted GSR computed by HDKR model instead of the general equation presented in [9].

The surface temperature from TIRS/Landsat-8 thermal data (band 10) was corrected, due temperature gradient caused by elevation, using a lapse rate coefficient derived by a linear regression between the surface temperature (T_s) and the pixel altitude.

117 The 24-hour actual evapotranspiration (ET_{24}) was calculated using a reference ET fraction
118 (ETrF) at time of Landsat overpass to extrapolate the instantaneous estimates of ET by SEBAL to
119 values for daily periods. The ETrF and ET_{24} was computed by equations 1 and 2:

$$ETrF = ET_{inst} / ET_0, \quad (1)$$

$$ET_{24} = ETrF \times ET_{0\ 24h}, \quad (2)$$

120 Where ET_{inst} is the hourly ET estimated by SEBAL, ET_0 and $ET_{0\ 24h}$ are the hourly and daily
121 alfalfa reference evapotranspiration computed by ASCE-Penman Monteith equation [12],
122 respectively. Both in the ET_0 and $ET_{0\ 24h}$ computations were used meteorological data from GLDAS
123 and solar radiation from the tilted GSR model.

124 3. Results

125 3.1. Spatial distribution of $GSR_{T\ 24}$ and ET_{24} over the terrain angles

126 In Paraibuna watershed the average value of $GSR_{T\ 24}$ obtained from the solar radiation model
127 was 313.6 $W.m^{-2}$ in summer, ranging from 78.9 to 346 $W.m^{-2}$. In winter the average value was 264.4
128 $W.m^{-2}$, ranging from 31.7 to 306 $W.m^{-2}$. The average ET_{24} obtained from the modified SEBAL, in
129 summer and winter, were 4,98 and 4,07 $mm.day^{-1}$, whereas the maximum average values were 5.48
130 and 5.10 $mm.day^{-1}$, respectively.

131 Table 2 and 3 shows the distribution of Mean and Coeficient of Variation (CV) of ET_{24} take into
132 account different slopes and azimuths of terrain in the two evaluated periods.

133 **Table 2.** Mean and CV of ET_{24} on different terrain slopes over Paraibuna watershed.

Terrain Slope		0 to 15°	15 to 30°	30 to 45°	above 45°
Summer	Mean (mm)	5.18	4.85	4.35	2.74
	CV (%)	2.10	6.04	12.82	24.95
Winter	Mean (mm)	4.78	4.35	3.71	2.43
	CV (%)	1.09	3.87	18.06	43.61

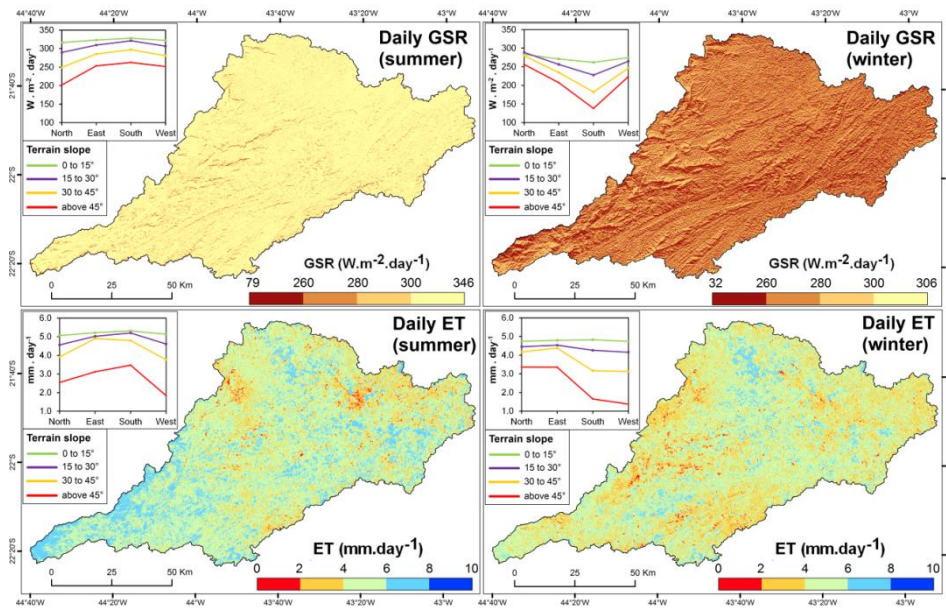
134 **Table 3.** Mean and CV of ET_{24} on different terrain azimuths over Paraibuna watershed.

Terrain Azimuth		315 to 45° (N)	45 to 135° (E)	135 to 225° (S)	225 to 315° (W)
Summer	Mean (mm)	4.31	4.85	4.94	4.24
	CV (%)	17.87	12.56	11.64	23.62
Winter	Mean (mm)	4.35	4.45	3.84	3.75
	CV (%)	9.52	9.48	26.99	28.58

135 On steeper slopes (above 45°) was found the higher variability (higher CV) of ET_{24} , with CV of
136 about 25% for summer and 43.6% in winter. In contrast, these areas showed the lowest mean values
137 of ET_{24} with 2.7 and 2.4 $mm.day^{-1}$ in summer and winter, respectively.

138 According to Figure 2 below, the $GSR_{T\ 24}$ and ET_{24} spatial distribution on the watershed showed
139 differences between the two periods, especially in areas with slopes above 45°. In summer the $GSR_{T\ 24}$
140 and ET_{24} distribution was more homogeneous with slightly higher values in Southern slopes, with
141 differences of 9.8% for ET_{24} . In contrast, in winter the highest ET_{24} values occurred on slopes facing
142 the North and East, while lowest ET_{24} values occurred on South and West, with average differences
143 about 10.6% and 11.9%, respectively.
144

145



146

147

Figure 2. GSR_{T24} and ET_{24} maps in summer (Left) and winter (Right) on the Paraibuna watershed.

148

3.2. Statistical relations between terrain angles, GSR_{T24} and ET_{24}

149

150

151

152

153

154

155

156

As shown in the plots of figure 3 below, both GSR_{T24} and ET_{24} values showed higher relationship with the terrain slope values, with negative correlation coefficient (r) of -0.82 (R^2 0.68) and -0.62 (R^2 0.39) for summer, and -0.54 (R^2 0.29) and -0.67 (R^2 0.45) for winter, respectively. In contrast, the correlation coefficient between GSR_{T24} and ET_{24} with the terrain azimuth values were weaker in both periods, with R^2 less than 0.1. In this selected areas was found a significant relation between GSR_{T24} and ET_{24} values, with a correlation coefficient of 0.68 (R^2 0.47) in summer and 0.65 (R^2 0.42) in winter.

157

158

159

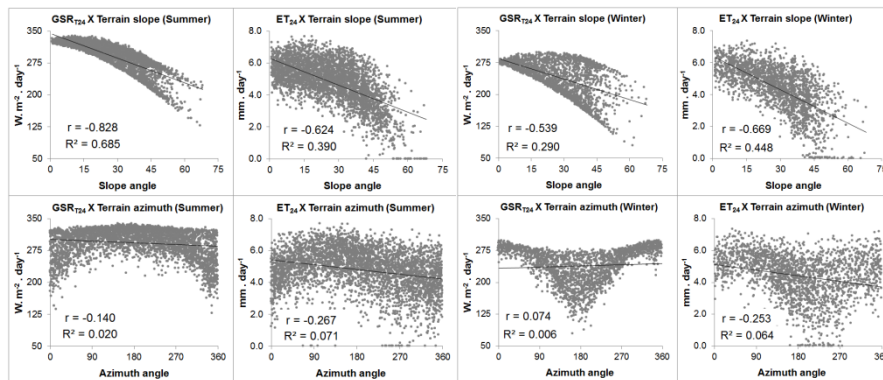


Figure 3. Distribution plot of GSR_{T24} and ET_{24} in relation to the Slope (Top) and Azimuth (Bottom), in non-flat forested areas (Slope $> 1^\circ$ and NDVI > 0.7).

160

4. Discussion

161

162

163

164

165

166

The notable spatial difference in GSR_{T24} and ET_{24} between the two evaluated periods can be explained in a way, by the significant influence of topography, mainly the slope angle, as showed by high coefficients of variation in slopes above 45° and the R^2 of distribution plots. In general, ET values follow the spatial distribution of GSR . However, average ET in slopes facing West showed inconsistent with average GSR values, especially in winter. This can occur due to some limitation in extrapolating from instantaneous to daily values using the reference ET fraction (ET_{RF}) at time of

167 Landsat overpass in mountainous areas. Another source of uncertainties is the relationship between
168 the terrain angles and the land surface temperature (LST). Future research should also investigate
169 the impact of topography on remotely sensed LST and ETrF and their influence on ET estimation
170 over this watershed. In addition, future field validation campaigns may better evaluate the
171 preliminary results of this study.

172 5. Conclusions

173 In this work the SEBAL adaptations for mountainous areas and the integration with a Solar
174 radiation model for tilted surfaces and the GLDAS meteorological dataset allowed a detailed capture
175 of the spatial variability of ET in the Paraibuna watershed without the use of ground data. The
176 analysis take into account different slopes and azimuths of terrain, wich can improve ET analysis in
177 a mountainous basins with scarcity ground-based data.

178 **Conflicts of Interest:** The authors declare no conflict of interest.

179 References

- 180 1. Gao, Y.C.; Long, D.; Li, Z.L. Estimation of daily actual evapotranspiration from remotely sensed data
181 under complex terrain over the upper Chao river basin in North China. *International Journal of Remote*
182 *Sensing* **2008**, *29*, 3295–3315.
- 183 2. Aguilar, C.; Herrero, J.; Polo, M.J. Topographic effects on solar radiation distribution in mountainous
184 watersheds and their influence on reference evapotranspiration estimates at watershed scale. *Hydrology*
185 *and Earth System Sciences (HESS)* **2010**, *14*, 2479–2494.
- 186 3. Chen, X.; Su, Z.; Ma, Y.; Yang, K.; Wang, B. Estimation of surface energy fluxes under complex terrain of
187 Mt. Qomolangma over the Tibetan Plateau. *Hydrology and Earth System Sciences* **2013**, *17*, 1607–1618.
- 188 4. Elhaddad, A.; Garcia, L.A. ReSET-Raster: Surface Energy Balance Model for Calculating
189 Evapotranspiration Using a Raster Approach. *Journal of Irrigation and Drainage Engineering* **2011**, *137*,
190 203–210.
- 191 5. NASA. LDAS Land Data Assimilation Systems. Available online: <https://ldas.gsfc.nasa.gov/gldas/>
192 (accessed on 12 Dec. 2017).
- 193 6. MAPBIOMAS. Project MapBiomass - Collection 2 of Brazilian Land Cover & Use Map Series. Available
194 online: <http://mapbiomas.org/> (accessed on 12 Dec. 2017).
- 195 7. Duffie, J. A. & Beckman, W. A. *Solar Engineering of Thermal Processes*. 4th ed.; John Wiley & Sons: Hoboken,
196 New Jersey, USA, 2013; 910 p.
- 197 8. Wong, L.T.; Chow, W.K. Solar radiation model. *Applied Energy* **2001**, *69*, 191–224.
- 198 9. Waters, R.; Allen, R.G.; Tasumi, M.; Trezza, R. *Surface energy balance algorithms for land. Idaho*
199 *Implementation. Advance training and users manual, version 1.0*, 2002; 98 p.
- 200 10. Tasumi, M.; Allen, R. G.; Trezza, R. At-surface reflectance and Albedo from satellite for operational
201 calculation of land surface energy balance. *Journal of Hydrologic Engineering*, **2008**, *13*, 51–63.
- 202 11. Soenen, S.A.; Peddle, D.R.; Coburn, C.A. SCS + C: A modified Sun-Canopy Sensor topographic correction
203 in forested terrain. *IEEE Transactions on Geoscience and Remote Sensing* **2005**, *43*, 2148–2159.
- 204 12. ASCE–EWRI. *The ASCE Standardized Reference Evapotranspiration Equation*. Report 0-7844-0805-X, ASCE
205 Task Committee on Standardization of Reference Evapotranspiration. Reston, Va., American Soc. Civil
206 Engineers, USA, 2005; 70 p.

207



© 2018 by the authors; licensee MDPI, Basel, Switzerland. This article is an open access article distributed under the terms and conditions of the Creative Commons Attribution (CC-BY) license (<http://creativecommons.org/licenses/by/4.0/>).